

The properties of D and D^* mesons in the nuclear medium

L. Tolós¹, C. García-Recio² and J. Nieves³

¹ Theory Group. KVI. University of Groningen,
Zernikelaan 25, 9747 AA Groningen, The Netherlands

² Departamento de Física Atómica, Molecular y Nuclear,
Universidad de Granada, E-18071 Granada, Spain

³ Instituto de Física Corpuscular (centro mixto CSIC-UV)
Institutos de Investigación de Paterna, Aptdo. 22085, 46071, Valencia, Spain
(Dated: December 19, 2018)

Abstract

We study the properties of D and D^* mesons in nuclear matter within a simultaneous self-consistent coupled-channel unitary approach that implements heavy-quark symmetry. The in-medium solution accounts for Pauli blocking effects, and for the D and D^* self-energies in a self-consistent manner. We pay a special attention to the renormalization of the intermediate propagators in the medium beyond the usual cutoff scheme. We analyze the behavior in the nuclear medium of the rich spectrum of dynamically-generated baryonic resonances in the $C = 1$ and $S = 0$ sector, and their influence in the self-energy and, hence, the spectral function of the D and D^* mesons. The D meson quasiparticle peak mixes with $\Sigma_c(2823)N^{-1}$ and $\Sigma_c(2868)N^{-1}$ states while the $\Lambda_c(2595)N^{-1}$ mode is present in the low-energy tail of the spectral function. The D^* spectral function incorporates $J = 3/2$ resonances, and $\Sigma_c(2902)N^{-1}$ and $\Lambda_c(2941)N^{-1}$ fully determine the behavior of D^* meson spectral function at the quasiparticle peak. As density increases, these resonant-hole modes tend to smear out and the spectral functions get broad. We also obtain the D and D^* scattering lengths, and optical potentials for different momentum and density regimes. The D meson potential stays attractive while the D^* meson one is repulsive with increasing momentum and densities up to twice that of the normal nuclear matter. Compared to previous in-medium SU(4) models, we obtain similar values for the real part of the D meson potential but much smaller imaginary parts. This result can have important implications for the observation of D^0 -nucleus bound states.

PACS numbers: 11.10.St, 12.38.Lg, 14.20.Lq, 14.40.Lb, 21.65.-f

I. INTRODUCTION

The interest on the properties of open and hidden charmed mesons was triggered more than 20 years ago in the context of relativistic nucleus-nucleus collisions in connection to the charmonium suppression [1] as a probe for the formation of Quark-Gluon Plasma (QGP). The experimental programme in hadronic physics of the future FAIR facility at GSI [2] will move from the light quark sector to the heavy one and will face new challenges where charm plays a dominant role. In particular, a large part of the PANDA physics programme will be devoted to charmonium spectroscopy. Moreover, the CBM experiment will extend the GSI programme for in-medium modification of hadrons in the light quark sector, and provide first insight into the charm-nucleus interaction.

The primary theoretical effort is to understand the interaction between hadrons with the charm degree of freedom. Charmed baryonic resonances have received recently a lot of attention motivated by the discovery of quite a few new states by the CLEO, Belle and BABAR collaborations [3, 4, 5, 6, 7, 8]. Whether those resonances have the usual qqq structure or qualify better as being dynamically generated via meson-baryon scattering processes is a matter of strong interest. In fact, the unitarization, in coupled-channels, of the chiral perturbation amplitudes for scattering of 0^- octet Goldstone bosons off baryons of the nucleon $1/2^+$ octet has proven to be quite successful in the charmless sector [9, 10, 11, 12, 13, 14, 15, 16, 17, 18, 19, 20, 21, 22, 23, 24, 25, 26, 27, 28]. The modification of the various meson-baryon amplitudes for the case of finite temperature and/or nuclear density has also attracted a lot of attention and has been carefully discussed [29, 30, 31, 32, 33, 34].

The extension to the charm sector of the unitarized meson-baryon method was attempted in a first exploratory work in Ref. [35], where the free space amplitudes were constructed from a set of separable coupled-channel interactions obtained from chirally motivated lagrangians upon replacing the s quark by the c quark. A different approach resulting from the scattering of Goldstone bosons off the ground state $1/2^+$ charmed baryons was pursued in [18], but the substantial improvement in constructing the meson-baryon interaction in the charm sector came from exploiting the universal vector-meson coupling hypothesis to break the $SU(4)$ symmetry [36]. The t -channel exchange of vector mesons (TVME) between pseudoscalar mesons and baryons preserved chiral symmetry in the light meson sector keeping the Weinberg-Tomozawa (WT) type of interaction. An extension to d -wave $J = 3/2^-$ resonances was developed in [37], while some modifications over the model of Ref. [36] were implemented in Ref. [38], both in the kernel and in the renormalization scheme. More recently, there have been attempts to construct the DN and $\bar{D}N$ interaction by incorporating the charm degree of freedom in the $SU(3)$ meson-exchange model of the Jülich group [39, 40].

Nuclear medium modifications were then incorporated in order to study the properties of charmed mesons in nuclear matter, and the influence of those modifications in the charmonium production rhythm at finite baryon densities. Possible variation of this rhythm might indicate the formation of the QGP phase of QCD at high densities. Previous works based on mean-field approaches provided important mass shifts for the D and \bar{D} meson masses [41, 42, 43, 44]. Some of those models have been recently revised [45, 46]. However, the spectral features of D mesons in symmetric nuclear matter were obtained for the first time in the exploratory work of Ref. [35], while finite temperature effects were incorporated later on in Ref. [47]. Afterwards, within the $SU(4)$ TVME model of Ref. [36], the properties of the (D, \bar{D}) and (D_s, \bar{D}_s) mesons were analyzed in [48], and in [38, 49]. In this latter reference, the kernel and the renormalization scheme employed in Ref. [36] were modified.

However, those $SU(4)$ TVME inspired models are not consistent with heavy-quark symmetry (HQS), which is a proper QCD spin-flavor symmetry that appears when the quark masses, such as the charm mass, become larger than the typical confinement scale. As a consequence of this

symmetry, the spin interactions vanish for infinitely massive quarks. Thus, heavy hadrons come in doublets (if the spin of the light degrees of freedom is not zero), which are degenerated in the infinite quark-mass limit. And this is the case for the D meson and its vector partner, the D^* meson.

In fact, the incorporation of vector mesons into the coupled-channel picture has been pursued very recently in the strange sector. On one hand, vector mesons have been incorporated within the hidden-gauge formalism. Within this scheme, a broad spectrum of new resonant meson-baryon states have been generated [50, 51, 52]. On the other hand, the WT meson-baryon chiral Lagrangian has been also extended to account for vector meson degrees of freedom by means of a scheme that starts from a $SU(6)$ spin-flavor symmetry Lagrangian and that incorporates some symmetry breaking corrections determined by physical masses and meson decay constants [53, 54, 55, 56]. The corresponding Bethe-Salpeter equation reproduces the previous $SU(3)$ -flavor WT results for the lowest-lying s - and d -wave, negative parity baryon resonances and gives new information on more massive states, as for example the $\Lambda(1800)$ or $\Lambda(2325)$ resonances. The extension of this scheme to four flavors, incorporating the charm degree of freedom, was carried out in Ref. [57] and it automatically incorporates HQS in the charm sector improving in this respect on the $SU(4)$ TVME models, since D and D^* mesons are thus consistently treated. One of the distinctive differences of this approach with respect to those that built in the $SU(4)$ TVME model can be drawn in the wave function content of the resonances. Thus, for instance, the dynamics of the lowest lying resonance $\Lambda_c(2595)$ is completely dominated by the DN channel in the $SU(4)$ TVME model of Ref. [36], while it turns out be largely a D^*N state within the $SU(8)$ scheme of Ref. [57]. Such differences might have also a direct influence on the dynamics at finite densities.

Thus in this work, we aim to investigate the nuclear medium effects in hadronic systems with charm one ($C = 1$) and no strangeness ($S = 0$) within the $SU(8)$ model derived in [57]. In particular, we study the dynamically-generated baryonic resonances in the free space as well as in the nuclear medium in order to analyze how the masses and widths are modified with density. We also study the D and D^* mesons self-energies in the nuclear medium, calculating their spectral functions for a variety of densities and kinematical situations and the corresponding optical potentials. A novelty of our work is that we simultaneously obtain, in a self-consistent manner, the D and D^* meson self-energies. We then compare our results with the previous ones obtained within $SU(4)$ TVME schemes and other more simple models [35, 38, 47, 48, 49], paying also an special attention to the regularization of the intermediate propagators in the medium beyond the cutoff method. The nuclear medium effects for hadronic scattering amplitudes and for hadrons propagators are of interest for the understanding and correct interpretation of the data obtained in heavy-ion collisions where the high nuclear densities reached can substantially change the properties of the involved hadrons.

II. FORMALISM: THE DN AND D^*N INTERACTION IN NUCLEAR MATTER

We will calculate the self-energy of the D and D^* mesons in nuclear matter from a self-consistent calculation in coupled channels that treats the heavy pseudoscalar and vector mesons on equal footing, as required by HQS. To incorporate HQS to the meson-baryon interaction we extend the WT meson-baryon lagrangian to the $SU(8)$ spin-flavor symmetry group [57]. We start from the traditional three flavor WT Lagrangian, which is not just $SU(3)$ symmetric but also chiral ($SU_L(3) \otimes SU_R(3)$) invariant. Symbolically, up to an overall constant, the WT interaction is

$$\mathcal{L}_{\text{WT}} = \text{Tr}([M^\dagger, M][B^\dagger, B]), \quad (1)$$

where mesons (M) and baryons (B) fall in the SU(3) representation **8**, which is the adjoint representation. The commutator indicates a t -channel coupling to the **8_a** (antisymmetric) representation. For the SU(8) spin-flavor symmetry, the mesons M fall now in the **63** (adjoint representation) and the baryons B are found in the **120**, which is fully symmetric. The group reductions

$$\begin{aligned} \mathbf{63} \otimes \mathbf{63} &= \mathbf{1} \oplus \mathbf{63}_s \oplus \mathbf{63}_a \oplus \mathbf{720} \oplus \mathbf{945} \oplus \mathbf{945}^* \oplus \mathbf{1232} \\ \mathbf{120} \otimes \mathbf{120}^* &= \mathbf{1} \oplus \mathbf{63} \oplus \mathbf{1232} \oplus \mathbf{13104} \end{aligned} \quad (2)$$

lead to a total of four different t -channel SU(8) singlet couplings, that can be used to construct s -wave meson-baryon interactions

$$\begin{aligned} &\left((M^\dagger \otimes M)_{\mathbf{1}} \otimes (B^\dagger \otimes B)_{\mathbf{1}}\right)_{\mathbf{1}}, \quad \left((M^\dagger \otimes M)_{\mathbf{63}_a} \otimes (B^\dagger \otimes B)_{\mathbf{63}}\right)_{\mathbf{1}}, \\ &\left((M^\dagger \otimes M)_{\mathbf{63}_s} \otimes (B^\dagger \otimes B)_{\mathbf{63}}\right)_{\mathbf{1}}, \quad \left((M^\dagger \otimes M)_{\mathbf{1232}} \otimes (B^\dagger \otimes B)_{\mathbf{1232}}\right)_{\mathbf{1}}. \end{aligned} \quad (3)$$

To ensure that the SU(8) amplitudes will reduce to those deduced from the SU(3) WT Lagrangian in the (**8₁**)meson-(**8₂**)baryon subspace (denoting the SU(3) multiplets of dimensionality \mathbf{n} and spin J by $\mathbf{n}_{\mathbf{2J+1}}$), we set all the couplings in Eq. (3) to be zero except for

$$\mathcal{L}_{\text{WT}}^{\text{SU}(8)} = \left((M^\dagger \otimes M)_{\mathbf{63}_a} \otimes (B^\dagger \otimes B)_{\mathbf{63}}\right)_{\mathbf{1}}, \quad (4)$$

which is the natural and unique SU(8) extension of the usual SU(3) WT Lagrangian. To compute the matrix elements of the SU(8) WT interaction, $\mathcal{L}_{\text{WT}}^{\text{SU}(8)}$, we use quark model constructions of hadrons with field theoretical methods to express everything in tensor representations as described in Appendix A of Ref. [57]. Thus, we get the tree level amplitudes (we use the convention $V = -\mathcal{L}$):

$$V_{ab}^{IJSC}(\sqrt{s}) = D_{ab}^{IJSC} \frac{\sqrt{s} - M}{2f^2} \left(\sqrt{\frac{E + M}{2M}} \right)^2, \quad (5)$$

where the last factor is due to the spinor normalization convention: $\bar{u}u = \bar{v}v = 1$, as in Refs. [20, 22]. In the above expression $IJSC$ are the meson-baryon isospin, total angular momentum, strangeness and charm quantum numbers, M (E) the common mass (CM energy) of the baryons placed in the **120** SU(8) representation, and D^{IJSC} a matrix in the coupled channel space (see Ref. [57]).

However, the SU(8) spin-flavor is strongly broken in nature. The breaking of SU(8) is twofold. On one hand, we take into account mass breaking effects by adopting the physical hadron masses in the tree level interactions of Eq. (5) and in the evaluation of the kinematical thresholds of different channels. On the other hand, we consider the difference between the weak non-charmed and charmed pseudoscalar and vector meson decay constants. Then, our tree level amplitudes now read

$$V_{ab}^{IJSC}(\sqrt{s}) = D_{ab}^{IJSC} \frac{2\sqrt{s} - M_a - M_b}{4f_a f_b} \sqrt{\frac{E_a + M_a}{2M_a}} \sqrt{\frac{E_b + M_b}{2M_b}}, \quad (6)$$

where M_a (M_b) and E_a (E_b) are, respectively, the mass and the CM energy of the baryon in the a (b) channel. We focus in the non-strange ($S = 0$) and singly charmed ($C = 1$) sector, where the DN and D^*N are embedded. In particular, we look at $I = 0$ and $I = 1$ channels for $J = 1/2$ and $J = 3/2$. The channels involved in the coupled-channel calculation are given in Table I, where below every channel we indicate its mass threshold, $M + m$, in MeV units. Compared to [57], we take $m_\Delta = 1232$ MeV, instead of the pole mass. As a consequence, resonances that couple strongly to channels with Δ component might slightly change its position and width, as the case of

$$I = 0, J = 1/2$$

$\Sigma_c \pi$	ND	$\Lambda_c \eta$	ND^*	$\Xi_c K$	$\Lambda_c \omega$	$\Xi'_c K$	ΛD_s
2591.6	2806.15	2833.97	2947.54	2965.11	3069.11	3072.51	3084.18
ΛD_s^*	$\Sigma_c \rho$	$\Lambda_c \eta'$	$\Sigma_c^* \rho$	$\Lambda_c \phi$	$\Xi_c K^*$	$\Xi'_c K^*$	$\Xi_c^* K^*$
3227.98	3229.05	3244.24	3293.46	3305.92	3361.11	3468.51	3538.01

$$I = 1, J = 1/2$$

$\Lambda_c \pi$	$\Sigma_c \pi$	ND	ND^*	$\Xi_c K$	$\Sigma_c \eta$	$\Lambda_c \rho$	$\Xi'_c K$	ΣD_s	$\Sigma_c \rho$	$\Sigma_c \omega$
2424.5	2591.6	2806.15	2947.54	2965.12	3001.07	3061.95	3072.52	3161.64	3229.05	3236.21
ΔD^*	$\Sigma_c^* \rho$	$\Sigma_c^* \omega$	ΣD_s^*	$\Xi_c K^*$	$\Sigma_c \eta'$	$\Xi'_c K^*$	$\Sigma_c \phi$	$\Sigma^* D_s^*$	$\Sigma_c^* \phi$	$\Xi_c^* K^*$
3240.62	3293.46	3300.62	3305.45	3361.11	3411.34	3468.51	3473.01	3496.87	3537.42	3538.01

$$I = 0, J = 3/2$$

$\Sigma_c^* \pi$	ND^*	$\Lambda_c \omega$	$\Xi_c^* K$	ΛD_s^*	$\Sigma_c \rho$	$\Sigma_c^* \rho$	$\Lambda_c \phi$	$\Xi_c K^*$	$\Xi'_c K^*$	$\Xi_c^* K^*$
2656.01	2947.54	3069.11	3142.01	3227.98	3229.05	3293.46	3305.92	3361.11	3468.51	3538.01

$$I = 1, J = 3/2$$

$\Sigma_c^* \pi$	ND^*	$\Lambda_c \rho$	$\Sigma_c^* \eta$	ΔD	$\Xi_c^* K$	$\Sigma_c \rho$	$\Sigma_c \omega$	ΔD^*	$\Sigma_c^* \rho$
2656.01	2947.54	3061.95	3065.48	3099.23	3142.02	3229.05	3236.21	3240.62	3293.46
$\Sigma_c^* \omega$	ΣD_s^*	$\Sigma^* D_s$	$\Xi_c K^*$	$\Xi'_c K^*$	$\Sigma_c \phi$	$\Sigma_c^* \eta'$	$\Sigma^* D_s^*$	$\Sigma_c^* \phi$	$\Xi_c^* K^*$
3300.62	3305.45	3353.06	3361.11	3468.51	3473.01	3475.75	3496.87	3537.42	3538.01

TABLE I: For each isospin IJ sector, all the involved baryon-meson channels are compiled, with their mass thresholds, $M + m$, in MeV shown below.

($I = 1, J = 1/2$) $\Sigma_c(2556)$ and ($I = 1, J = 3/2$) $\Sigma_c(2554)$, few MeV's above the values in Ref. [57]. We also take $m_{K^*} = 892$ MeV. Besides, we also use experimental, when possible, or theoretical estimates for the meson decay constants. The used values in this work can be found in Table II of Ref. [57].

With the kernel of the meson-baryon interaction given in Eq. (6), we obtain the coupled DN and D^*N effective interaction in free space by solving the on-shell Bethe-Salpeter equation [11, 14, 15, 22, 58, 59]

$$T^{IJ}(\sqrt{s}) = \frac{1}{1 - V^{IJ}(\sqrt{s}) G^0(IJ)(\sqrt{s})} V^{IJ}(\sqrt{s}) , \quad (7)$$

in the coupled channel space. Here $G^0(IJ)(\sqrt{s})$ is a diagonal matrix consisting of loop functions. The free space loop function for channel a reads

$$G_a^0(IJ)(\sqrt{s}) = i2M_a \int \frac{d^4 q}{(2\pi)^4} D_{\mathcal{B}_a}^0(P - q) D_{\mathcal{M}_a}^0(q) , \quad (8)$$

$$D_{\mathcal{B}_a}^0(P - q) = ((P - q)^2 - M_a^2 + i\varepsilon)^{-1} , \quad (9)$$

$$D_{\mathcal{M}_a}^0(q) = (q^2 - m_a^2 + i\varepsilon)^{-1} , \quad (10)$$

where $s = P^2$, D^0 is a free hadron propagator, a runs for the allowed baryon-meson channels for the given IJ sector, and M_a and m_a are the masses of the baryon \mathcal{B}_a and meson \mathcal{M}_a in the channel a , respectively. The previously defined loop function is ultraviolet (UV) divergent. However, the

difference $G^0(\sqrt{s_1}) - G^0(\sqrt{s_2})$ is finite for any finite values of s_1 and s_2 , hence, the function can be regularized by setting a finite value of G^0 at a given point. We choose

$$G_a^{0(IJ)}(\sqrt{s} = \mu_a^{IJ}) = 0, \quad (11)$$

with index a running in the coupled channel space, as done in Refs. [36, 37, 57]. In those works, the subtraction point was taken to be independent of a and J as

$$(\mu^I)^2 = \alpha (m_{\text{th}}^2 + M_{\text{th}}^2), \quad (12)$$

where m_{th} and M_{th} are the meson and baryon masses of the hadronic channel with lowest mass threshold for a fixed I and arbitrary J . The value of $\alpha = 0.9698$ was adjusted to reproduce the position of the well established $\Lambda_c(2595)$ resonance with $IJ = (0, 1/2)$. Then, the same value will be used in all other sectors. In this work we will follow the same prescription, taking $(\mu^{I=0})^2 = \alpha(M_{\Sigma_c}^2 + m_\pi^2)$ and $(\mu^{I=1})^2 = \alpha(M_{\Lambda_c}^2 + m_\pi^2)$.

Hence, the renormalized (finite) loop function finally reads:

$$G^0(\sqrt{s}) = i2M \int \frac{d^4q}{(2\pi)^4} \left(D_{\mathcal{B}}^0(P - q) D_{\mathcal{M}}^0(q) - D_{\mathcal{B}}^0(\bar{P} - q) D_{\mathcal{M}}^0(q) \right), \quad (13)$$

with P and \bar{P} defined such that $P^2 = s$, $\bar{P}^2 = (\mu^I)^2$, where, for simplicity, the obvious isospin I , spin J and channel a labels have been omitted. This is the (standard) method we use to renormalize the free baryon-meson loop.

The properties of D and D^* mesons in nuclear matter are obtained by incorporating the corresponding medium modifications in the effective DN and D^*N interactions. One of the sources of density dependence comes from the Pauli principle acting on the nucleons. Another source is related to the change of the properties of mesons and baryons in the intermediate states due to the interaction with nucleons of the Fermi sea.

Those changes are implemented by using the in-medium hadron propagators instead of the corresponding free ones. Therefore, we should define a consistent renormalization scheme, similar to that adopted in the free case, for the loop function in a nuclear medium with density ρ .

Let us first review what has been done before. The in-medium loop function, G_Λ^ρ , used in Refs. [38, 49], depends on a regularization cutoff Λ that renders the UV divergence finite, and it is defined as:

$$G_\Lambda^\rho(P) = i2M \int_\Lambda \frac{d^4q}{(2\pi)^4} D_{\mathcal{B}}^\rho(P - q) D_{\mathcal{M}}^\rho(q), \quad (14)$$

where $D_{\mathcal{B}}^\rho$, $D_{\mathcal{M}}^\rho$ are the hadron propagators in a medium with density ρ . In those works [38, 49], the three-momentum cutoff Λ is fixed in such a way that the free ($\rho = 0$) results reproduce certain known experimental results (for instance, the position of the resonance $\Lambda_c(2595)$ for the sector with quantum numbers $IJSC = 0, 1/2, 0, 1$). This way of regularizing the UV loop function induces medium corrections of the type:

$$\begin{aligned} G_\Lambda^\rho(P) &= G_\Lambda^0(\sqrt{s}) + \delta G_\Lambda^\rho(P), \\ \delta G_\Lambda^\rho(P) &\equiv G_\Lambda^\rho(P) - G_\Lambda^0(\sqrt{s}) = i2M \int_\Lambda \frac{d^4q}{(2\pi)^4} \left(D_{\mathcal{B}}^\rho(P - q) D_{\mathcal{M}}^\rho(q) - D_{\mathcal{B}}^0(P - q) D_{\mathcal{M}}^0(q) \right) \end{aligned} \quad (15)$$

In this work, we do want to avoid finite-cutoff effects. So we define the in-medium loop function as the free one G^0 , given in Eq. (13) and defined as in Refs. [36, 37, 53, 55, 56, 57] without having

to introduce any cutoff, plus a term that accounts for the same kind of medium effects as those displayed in Eq. (15), but taking Λ large enough (that is $\Lambda \rightarrow \infty$). Hence, we will use:

$$G^\rho(P) = G^0(\sqrt{s}) + \delta G^\rho(P) ,$$

$$\delta G^\rho(P) = \lim_{\Lambda \rightarrow \infty} \delta G_\Lambda^\rho(P) \equiv i2M \int \frac{d^4 q}{(2\pi)^4} \left(D_B^\rho(P-q) D_{\mathcal{M}}^\rho(q) - D_B^0(P-q) D_{\mathcal{M}}^0(q) \right) . \quad (16)$$

The UV finite δG^ρ correction contains all the nuclear medium effects affecting the loop, and it is independent of the selected subtracting point used to regularize it. Then, a cutoff is not needed for the calculation. The defined loop function at finite density, G^ρ , can be rewritten as

$$G^\rho(P) = i2M \int \frac{d^4 q}{(2\pi)^4} \left(D_B^\rho(P-q) D_{\mathcal{M}}^\rho(q) - D_B^0(\bar{P}-q) D_{\mathcal{M}}^0(q) \right) , \quad (17)$$

where the integrand is the difference between two terms. The first one corresponds to the baryon and meson propagators calculated at density ρ and total momentum P . The second term depends neither on the density nor on P , and it is constructed out of propagators evaluated at $\rho = 0$ and with fixed total momentum \bar{P} , such that $\bar{P}^2 = (\mu^I)^2$. This shows that our prescription of Eq. (16) for G^ρ amounts to assume that the employed subtraction to make the UV divergent function finite is independent of the nuclear density.

For practical numerical purposes we will calculate G^ρ as specified in Eq. (16), where the free part is analytical, regularized with a subtracting constant and well known, and the medium modification part δG^ρ is numerically evaluated in the same way as done in previous works for G_Λ^ρ , but taking into account that it has a subtracting part G^0 providing a δG^ρ that is UV finite.

For the DN and D^*N channels, we consider Pauli blocking effects on the nucleons together with self-energy insertions of the D and D^* mesons. The self-energy is obtained self-consistently from the in-medium DN and D^*N effective interactions, $T^\rho_{D(D^*)N}$, as we will show in the following. The corresponding in-medium single-particle propagators are given by:

$$D_N^\rho(p) = \frac{1}{2E_N(\vec{p})} \left(\frac{1 - n(\vec{p})}{p^0 - E_N(\vec{p}) + i\varepsilon} + \frac{n(\vec{p})}{p^0 - E_N(\vec{p}) - i\varepsilon} + \frac{1}{-p^0 - E_N(\vec{p}) + i\varepsilon} \right)$$

$$= D_N^0(p) + 2\pi i n(\vec{p}) \frac{\delta(p^0 - E_N(\vec{p}))}{2E_N(\vec{p})} , \quad (18)$$

$$D_{D(D^*)}^\rho(q) = \left((q^0)^2 - \omega(\vec{q})^2 - \Pi_{D(D^*)}(q) \right)^{-1} = \int_0^\infty d\omega \left(\frac{S_{D(D^*)}(\omega, \vec{q})}{q^0 - \omega + i\varepsilon} - \frac{S_{\bar{D}(\bar{D}^*)}(\omega, \vec{q})}{q^0 + \omega - i\varepsilon} \right) , \quad (19)$$

where $E_N(\vec{p}) = \sqrt{\vec{p}^2 + M_N^2}$, $\omega(\vec{q}) = \sqrt{\vec{q}^2 + m_{D(D^*)}^2}$, $\Pi_{D(D^*)}(q^0, \vec{q})$ is the $D(D^*)$ meson self-energy and $S_{D(D^*)}$ the corresponding meson spectral function. In a very good approximation the spectral function for \bar{D} can be approximated by the free-space one, viz. by a delta function, because for that case $C = -1$, there are no low-lying baryon resonances. Finally, $n(\vec{p})$ is the Fermi gas nucleon momentum distribution, given by the step function $n(\vec{p}) = H(k_F - |\vec{p}|)$, with $k_F = (3\pi^2\rho/2)^{1/3}$.

Using Eq. (16) and performing the energy integral over q^0 , the DN and D^*N loop functions read

$$G^\rho_{D(D^*)N}(P) = G^0_{D(D^*)N}(\sqrt{s}) + \int \frac{d^3 q}{(2\pi)^3} \frac{M_N}{E_N(\vec{p})} \left[\frac{-n(\vec{p})}{(P^0 - E_N(\vec{p}))^2 - \omega(\vec{q})^2 + i\varepsilon} + \right. \quad (20)$$

$$\left. (1 - n(\vec{p})) \left(\frac{-1/(2\omega(\vec{q}))}{P^0 - E_N(\vec{p}) - \omega(\vec{q}) + i\varepsilon} + \int_0^\infty d\omega \frac{S_{D(D^*)}(\omega, \vec{q})}{P^0 - E_N(\vec{p}) - \omega + i\varepsilon} \right) \right] \Big|_{\vec{p}=\vec{P}-\vec{q}} ,$$

where the first term of the integral, proportional to $-n(\vec{p})$, is just what we call Pauli correction and accounts for the case where the Pauli blocking on the nucleon is considered and the meson in-medium selfenergy is neglected. The second term, proportional to $(1 - n(\vec{p}))$, is exactly zero if the meson spectral functions $S_{D(D^*)}$ were taken to be the free one, $S_{D(D^*)}^{\text{free}}(\omega, \vec{q}) = \delta(\omega - \omega(\vec{q})) / (2\omega)$. Then, it accounts for the contribution of the in-medium meson modification to the loop function. Note that, compared to the Refs. [38, 49], we also include the antiparticle contributions in the propagators.

As for $D\Delta$ and $D^*\Delta$ channels, we include the self-energy of the D and D^* mesons. Then, the equivalent of Eq. (20) for those channels read

$$G_{D(D^*)\Delta}^\rho(P) = G_{D(D^*)\Delta}^0(\sqrt{s}) + \int \frac{d^3q}{(2\pi)^3} \frac{M_\Delta}{E_\Delta(\vec{p})} \left(\frac{-1/(2\omega(\vec{q}))}{P^0 - E_\Delta(\vec{p}) - \omega(\vec{q}) + i\varepsilon} + \int_0^\infty d\omega \frac{S_{D(D^*)}(\omega, \vec{q})}{P^0 - E_\Delta(\vec{p}) - \omega + i\varepsilon} \right) \Big|_{\vec{p}=\vec{P}-\vec{q}}. \quad (21)$$

For the other channels that couple to DN and D^*N (see Table I), we refrain from including any medium modifications in the loop function and, therefore, we use the free-space one given in Eq. (13). This is due to the lack of knowledge on how the properties of some mesons, such as ρ or ω , change in the medium. Only pions in nuclear matter have been intensively studied [60, 61], but, as indicated in Ref. [57] and discussed in the next section, the coupling to intermediate states with pions is of minor importance for the dynamical generation of the baryon resonances in the $S = 0$ and $C = 1$ sector that governs the DN and D^*N dynamics in nuclear matter.

We can now solve the on-shell Bethe-Salpeter equation in nuclear matter for the in-medium amplitudes

$$T^{\rho(IJ)}(P) = \frac{1}{1 - V^{IJ}(\sqrt{s}) G^{\rho(IJ)}(P)} V^{IJ}(\sqrt{s}). \quad (22)$$

The in-medium D and D^* self-energies are finally obtained by integrating $T^{\rho}_{D(D^*)N}$ over the nucleon Fermi sea,

$$\Pi_D(q^0, \vec{q}) = \int \frac{d^3p}{(2\pi)^3} n(\vec{p}) \left[T^{\rho(I=0, J=1/2)}_{DN}(P^0, \vec{P}) + 3T^{\rho(I=1, J=1/2)}_{DN}(P^0, \vec{P}) \right], \quad (23)$$

$$\begin{aligned} \Pi_{D^*}(q^0, \vec{q}) = \int \frac{d^3p}{(2\pi)^3} n(\vec{p}) & \left[\frac{1}{3} T^{\rho(I=0, J=1/2)}_{D^*N}(P^0, \vec{P}) + T^{\rho(I=1, J=1/2)}_{D^*N}(P^0, \vec{P}) \right. \\ & \left. + \frac{2}{3} T^{\rho(I=0, J=3/2)}_{D^*N}(P^0, \vec{P}) + 2T^{\rho(I=1, J=3/2)}_{D^*N}(P^0, \vec{P}) \right], \quad (24) \end{aligned}$$

where $P^0 = q^0 + E_N(\vec{p})$ and $\vec{P} = \vec{q} + \vec{p}$ are the total energy and momentum of the DN (D^*N) pair in the nuclear matter rest frame and the values (q^0, \vec{q}) stand for the energy and momentum of the D and D^* meson also in this frame. The $\Pi_{D(D^*)}(q^0, \vec{q})$ has to be determined self-consistently since it is obtained from the in-medium amplitude $T^{\rho}_{D(D^*)N}$ which contains the $D(D^*)N$ loop function $G^{\rho}_{D(D^*)N}$, and this last quantity itself is a function of $\Pi_{D(D^*)}(q^0, \vec{q})$. From this we obtain the corresponding spectral function to complete the integral for the loop function $G^{\rho}_{D(D^*)(N, \Delta)}(P^0, \vec{P})$ as given in Eqs. (20,21).

III. RESULTS

We start this section by displaying in Fig. 1 the squared amplitude of the $D^*N \rightarrow D^*N$ transition for different partial waves as a function of the center-of-mass energy P^0 for a total momentum $|\vec{P}| = 0$. In particular, we show certain partial waves and energy regimes where we

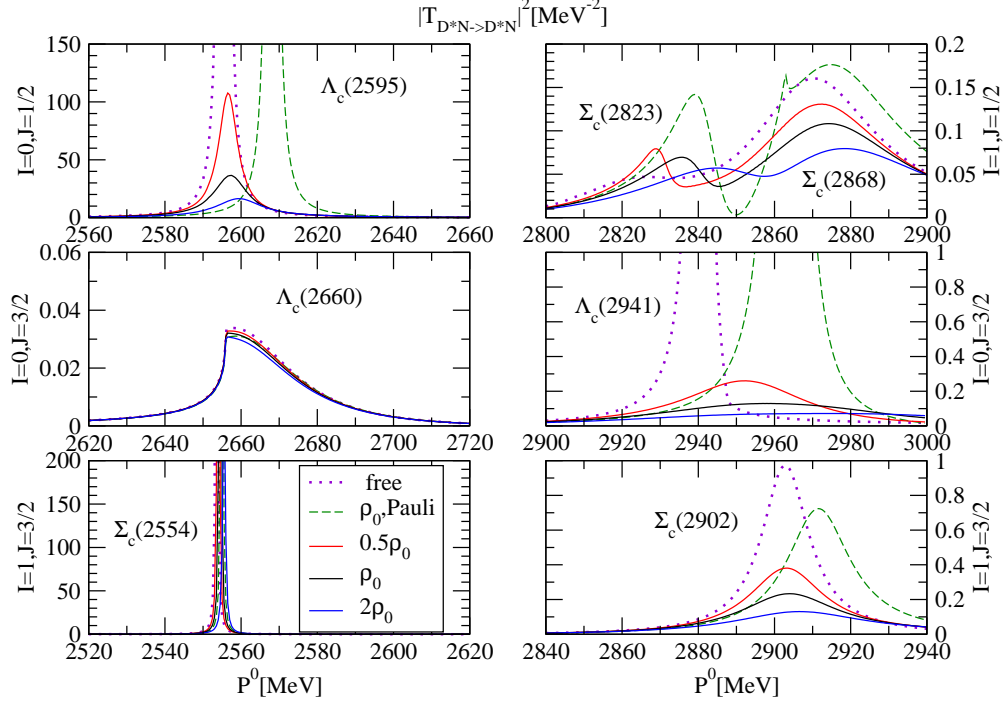


FIG. 1: Squared of the $D^*N \rightarrow D^*N$ amplitude for different partial waves as function of the center-of-mass energy P^0 for fixed total momentum $|\vec{P}| = 0$. Several resonances are shown: $(I = 0, J = 1/2)$ $\Lambda_c(2595)$, $(I = 1, J = 1/2)$ $\Sigma_c(2823)$ and $\Sigma_c(2868)$, $(I = 0, J = 3/2)$ $\Lambda_c(2660)$, $(I = 0, J = 3/2)$ $\Lambda_c(2941)$, $(I = 1, J = 3/2)$ $\Sigma_c(2554)$ and $(I = 1, J = 3/2)$ $\Sigma_c(2902)$.

can find seven resonances predicted by the SU(8) model [57] that have or can have experimental confirmation [62], i.e., $(I = 0, J = 1/2)$ $\Lambda_c(2595)$, $(I = 1, J = 1/2)$ $\Sigma_c(2823)$ and $\Sigma_c(2868)$, $(I = 0, J = 3/2)$ $\Lambda_c(2660)$, $(I = 0, J = 3/2)$ $\Lambda_c(2941)$, $(I = 1, J = 3/2)$ $\Sigma_c(2554)$ and $(I = 1, J = 3/2)$ $\Sigma_c(2902)$ resonances. All of them couple to the D^*N despite not being the dominant one for $\Lambda_c(2660)$, $\Sigma_c(2823)$ and $\Sigma_c(2554)$, as discussed in Ref. [57]. However, we choose to display these amplitudes for different nuclear densities, since they determine the D^* self-energy, as follows from Eq. (24). We analyze three different cases: (i) solution of the on-shell Bethe-Salpeter equation in free space (dotted lines), which was already studied in Ref. [57], (ii) in-medium calculation of the on-shell Bethe-Salpeter including Pauli blocking on the nucleon intermediate states at normal nuclear matter density $\rho_0 = 0.17 \text{ fm}^{-3}$ (dashed lines), (iii) in-medium solution which incorporates Pauli blocking effects and the D and D^* self-energies in a self-consistent manner for three densities, ranging from 0.5 to 2 ρ_0 (solid lines).

The $\Lambda_c(2595)$ resonance is predominantly a D^*N bound state in contrast to SU(4) TVME model, where it emerged as a DN quasi-bound state [18, 36, 37, 38, 48, 49]. Pauli blocking effects on the intermediate nucleon states move the resonance to higher energies, as already found in previous in-medium models [35, 38, 48], due to the restriction of available phase space in the unitarization procedure. The shift in mass is of the order of 12 MeV, while for the SU(4) TVME model of Ref. [38] the shift is around a factor of two larger. This change in the energy shift provided by Pauli blocking can be attributed either to the different SU(4) and SU(8) kernels, or to the renormalization scheme employed to make finite the loop function or the combination of both effects. In order to disentangle between them, we study in Fig. 2 the $\Lambda_c(2595)$ resonance in the $DN \rightarrow DN$ transition by using the SU(4) TVME model (with $\Sigma_{DN}=0$) of Ref. [38] for cases

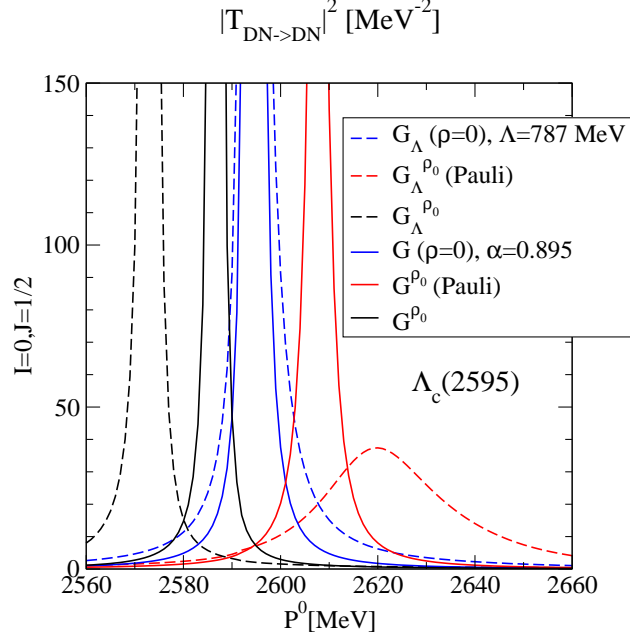


FIG. 2: Squared of the $DN \rightarrow DN$ amplitude in $(I = 0, J = 1/2)$ $\Lambda_c(2595)$ channel as function of the center-of-mass energy P^0 with $|\vec{P}| = 0$. We show results obtained with the SU(4) TVME model with a three-momentum cutoff, as in Ref. [38], and for comparison, we also show results using the renormalization scheme assumed in this work [Eqs. (16,17)]. We examined three different cases: free amplitude, calculation including Pauli blocking effects at $\rho = \rho_0$ and in-medium self-consistent solution at ρ_0 .

(i) to (iii) above. We compare results obtained by using the cutoff regularization [38] and our new renormalization scheme [Eqs. (16,17)]¹. A similar mass shift for the $\Lambda_c(2595)$ is observed in both SU(4) and SU(8) models when Pauli blocking effects are included for the new renormalization scheme. Therefore, we conclude that the different renormalization of the loop function is the main source of discrepancy, i.e., the in-medium solution depends strongly on the correct treatment of the \sqrt{s} dependence of the loop function. The treatment proposed here clearly improves over those based on the use of a cutoff. Thus, the resonances which are far offshell from their dominant channel will be heavily affected, as in the case of $\Lambda_c(2595)$. The self-consistent procedure moves the resonance closer to the free position because the repulsive effect of the Pauli blocking is tamed by the inclusion of the D and D^* self-energies. In this case, the difference between SU(8) and SU(4) models is not only due to the renormalization scheme but also to the inclusion of the D^* self-energy, which compensates the attraction felt by the D mesons, as we will see in the next figures.

The $(I = 1, J = 1/2)$ $\Sigma_c(2823)$ and $\Sigma_c(2868)$ are shown in the top right panel of Fig. 1. Although no experimental evidence of those resonances is available yet, they lie very close to the DN threshold and, therefore, changes in the nuclear medium will have an important effect on the D self-energy, which is a matter of interest in this work. In fact, those resonant states are significantly modified in the medium, since both resonances couple significantly to DN and D^*N systems as well as $D^*\Delta$ and any medium modification in those systems alters their behavior.

The next resonance predicted by the SU(8) model [57], the $(I = 0, J = 3/2)$ $\Lambda_c(2660)$, might be identified with the experimental $\Lambda_c(2625)$, which is the charm counterpart of the $\Lambda(1520)$. This

¹ We fix now $\alpha = 0.895$ to obtain the correct position of $\Lambda_c(2595)$

state couples strongly to the $\Sigma_c^* \pi$ channel and more weakly to the $D^* N$ pair. Pauli blocking and self-consistency have smaller effects than in the case of the $\Lambda_c(2595)$ resonance. This is because, while the $\Lambda_c(2595)$ resonance varies in the medium due to the changes affecting its two dominant channels, $D^* N$ and DN , the $\Lambda_c(2660)$ is only modified via the secondary $D^* N$ channel. We do not include any medium modifications affecting to its dominant channel, $\pi \Sigma_c^*$. Though the pion self-energy [60, 61] may induce some changes in this resonance, the expected effect of those modifications in the D and D^* self-energies are minor. On one hand, this partial wave will only have a direct contribution to the D^* self-energy, and thus the D self-energy will be affected indirectly via the simultaneous self-consistent calculation of the D and D^* self-energies. On the other hand, the effect of this resonance in the D^* self-energy is marginal because it only reflects in the low-energy tail, far from the quasiparticle peak. Then, we refrain to introduce any medium changes for this channel.

The $(I = 0, J = 3/2)$ $\Lambda_c(2941)$ resonance might be a candidate for the experimental $\Lambda_c(2940)$, which J^P is unknown [62]. This correspondence is made under the assumption that our model needs an additional implementation of p -wave interactions in order to explain the decay into $D^0 p$ pairs reported in Ref. [7], which is also hinted by the dominant coupling to $D^* N$. This strong coupling changes its properties significantly when medium modifications are implemented. Moreover, the fact that the $\Lambda_c(2941)$ lies so close to the $D^* N$ threshold will have important consequences on the D^* self-energy and, hence, on the spectral function, as we will see in the following.

The $(I = 1, J = 3/2)$ $\Sigma_c(2554)$ resonance has not yet a experimental confirmation. However, similarly to the $\Lambda_c(2660)$, this resonance might be the counterpart in the charm sector of the $\Sigma(1670)$. It couples strongly to $D\Delta$ and $D^*\Delta$ channels, which correspond to the $\bar{K}\Delta$ in the strange sector. Pauli blocking effects on the nucleons are relatively weak because the coupling to the $D^* N$ channel is approximately half the coupling to the two dominant channels. Changes due to the selfconsistent procedure are comparable to the case of the $\Lambda_c(2660)$.

The $\Sigma_c(2902)$ resonance in the $(I = 1, J = 3/2)$ sector can be a candidate for the $\Sigma_c(2800)$ resonance, by varying slightly the renormalization scale and if this resonance could be also seen in $\pi\pi\Lambda_c$ states [57]. This is in contrast with SU(4) TVME models, which predict it in the $I = 1, J = 1/2$ channel [36, 37, 38, 48]. With regard to medium effects, those are comparable to the $\Lambda_c(2595)$ case. The dominant channel for the generation of this resonance is $D^* N$. Moreover, this resonance lies 50 MeV below the $D^* N$ threshold. Therefore, modifications due to Pauli blocking and self-consistency are expected to be more important than for $\Lambda_c(2660)$ and $\Sigma_c(2554)$, and turn out to be comparable to the changes in $\Lambda_c(2595)$.

We show next in the left and right panels of Fig. 3 the D and D^* self-energies, respectively, as functions of the meson energy q^0 . The D and D^* self-energies result from the integration over the DN and $D^* N$ amplitudes, respectively, after self-consistency is reached simultaneously. In the upper panels we display the real part of the self-energies for ρ_0 at meson zero momentum (solid lines) together with the partial wave decomposition (dashed and dash-dotted lines). The partial waves weighted by the corresponding factors in Eqs. (23) and (24) are summed up in order to obtain the total self-energies. In the lower panels we show the imaginary part of the self-energies for densities ranging from $0.5 \rho_0$ to $2 \rho_0$ and $q = 0$ MeV/c (solid lines) as well as the result for ρ_0 and $q = 450$ MeV/c (dashed lines). The dotted vertical lines in the upper panels indicate the free D and D^* meson masses.

With regard to the D meson self-energy, we observe that in the $I = 0, J = 1/2$ partial wave the contribution of the $\Lambda_c(2595)$ resonance clearly appears for energies of the D meson around 1650 MeV, while the resonant state $\Sigma_c(2556)$ governs the $I = 1, J = 1/2$ partial wave around $q^0 = 1615$ MeV. This state couples mostly to $D^* \Delta$, mixed with DN and $D_s^* \Sigma^*$, and it is absent in the SU(4) models [18, 36, 37, 38, 48], which do not include channels with a vector meson and a $3/2^+$ baryon. Close to the DN threshold ($\sqrt{s} = 2806$ MeV in free space), the $I = 1, J = 1/2$

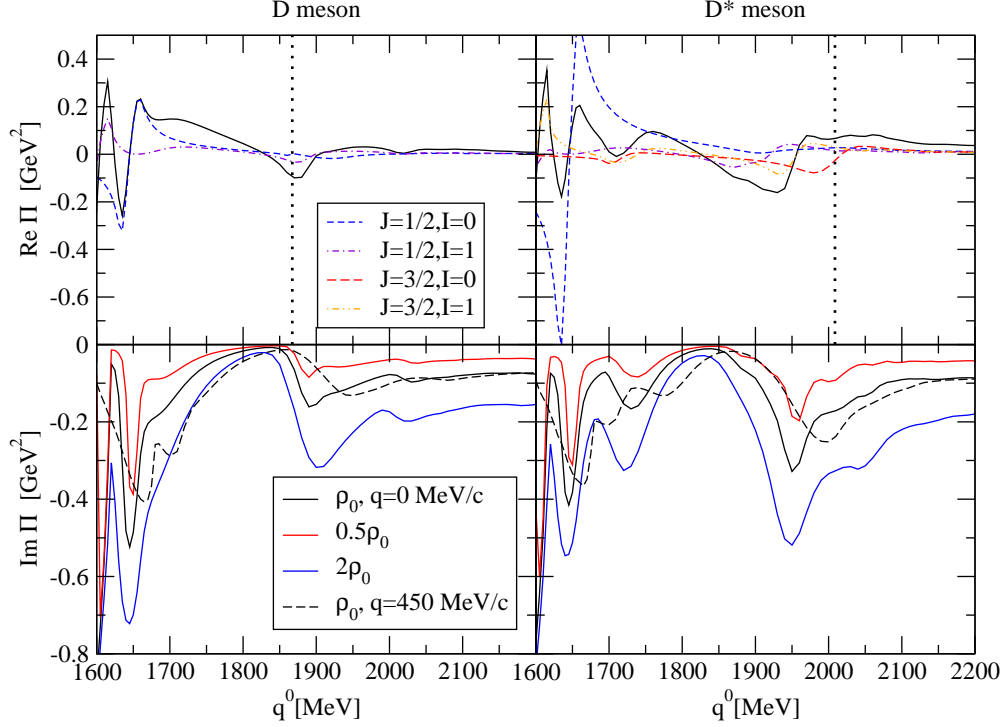


FIG. 3: Real and imaginary parts of the D and D^* self-energies as functions of the meson energy q^0 , including the decomposition in partial waves (first row), and for different densities and momenta (second row). The positions of the D and D^* meson masses are also shown as vertical lines for reference.

is the dominant partial wave. This is a consequence of the fact that this threshold lies very close to a resonant state in the sector $I = 1, J = 1/2$ of 2823 MeV with a width of $\Gamma = 35$ MeV. This resonance is affected by Pauli blocking and self-consistency, i.e., by the nuclear medium, as it couples strongly to states with D , D^* and nucleon content. Closer to that structure, we also found a very narrow state in $I = 0, J = 1/2$ with a mass of 2821 MeV. This resonant state is less modified in the medium, since it couples marginally to the DN channel. Due to its narrow width even in nuclear matter, the main contribution to the D meson self-energy close to the DN threshold comes from the $J = 1/2$ $\Sigma_c(2823)$ resonance but modified by the near resonance $J = 1/2$ $\Sigma_c(2868)$. Those resonances lie above the DN threshold and, hence, have an attractive effect at the DN threshold.

The imaginary part of the D meson self-energy, in absolute value, grows with increasing density because of an enhancement of collision and absorption processes, while for a finite momentum of $q = 450$ MeV/c, the resonant-hole structures that configure the self-energy dilute and slightly move to higher energies. The change in density and momentum can be seen more easily in the spectral function, as we will show below in Fig. 4. Compared to previous results in nuclear matter [35, 38, 47, 48, 49], the density and momentum dependence of the D meson self-energy are qualitatively similar. However, in the SU(8) model, we have a richer spectrum of resonant states which is reflected in the self-energy. While the $\Lambda_c(2595)N^{-1}$ and $\Sigma_c(2800)N^{-1}$ determine the D meson self-energy in SU(4) models [38, 48], those contributions together with few other resonant-hole states around $q^0 = 1860 - 2060$ MeV, such as $\Sigma_c(2823)N^{-1}$ and $\Sigma_c(2868)N^{-1}$, clearly manifest also in the D self-energy using the SU(8) interaction [57].

A novelty of the SU(8) model is that it allows to simultaneously obtain the D and D^* self-energies. The D^* self-energy comes from the contribution not only from the $J = 1/2$ partial

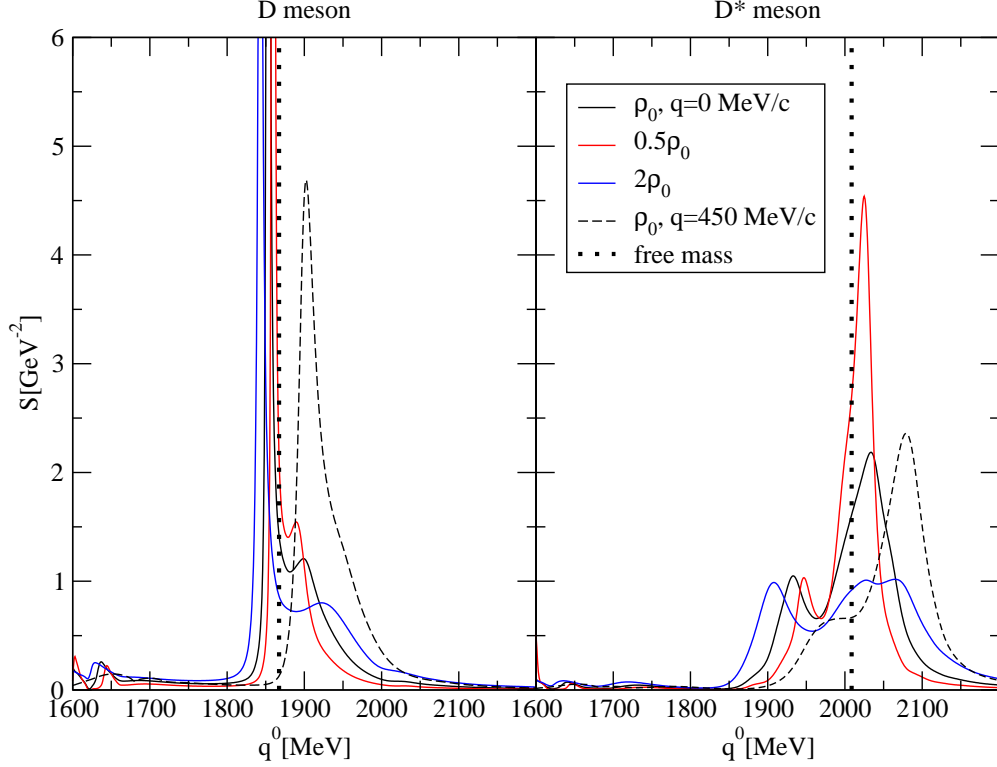


FIG. 4: D and D^* spectral functions as function of the meson energy q^0 for different densities and two different three momenta. The positions of the D and D^* meson free masses are also shown for reference (dotted vertical lines).

waves but also from the $J = 3/2$ ones of the D^*N amplitude. As expected in the $J = 1/2$ sector, we find the $\Lambda_c(2595)N^{-1}$ and $\Sigma_c(2556)N^{-1}$ components for $q^0 = 1650$ MeV and $q^0 = 1615$ MeV, respectively. For higher energies around $q^0 = 1880 - 1930$ we see the $\Sigma_c(2823)N^{-1}$ and $\Sigma_c(2868)N^{-1}$ contributions. In the $J = 3/2$ sector, we find $\Sigma_c(2554)N^{-1}$ for $q^0 = 1610$ MeV. Close to the D^*N threshold ($\sqrt{s} = 2947$ MeV in free space), around $q^0 = 1960$ MeV, the $\Sigma_c(2902)N^{-1}$ excitation becomes dominant. This resonant-hole state mixes with $\Lambda_c(2941)N^{-1}$. The combination of both $J = 3/2$ resonances becomes the dominant contribution close to D^*N threshold and has a repulsive effect in the D^* self-energy, as observed in the upper right panel. Density and finite momentum have a similar outcome as in the case of the D self-energy. Those effects are better visualized with the spectral function.

The spectral functions for D and D^* mesons as function of the meson energy q^0 are displayed in the left and right panels of Fig. 4, respectively. The solid lines correspond to the spectral functions at zero momentum from $0.5 \rho_0$ to $2 \rho_0$ for $|\vec{q}| = 0$ MeV/c. At ρ_0 we also show the spectral functions for $|\vec{q}| = 450$ MeV/c (dashed lines). A dotted vertical line indicating the free D and D^* meson masses is also drawn for reference.

The quasiparticle peak of the spectral function, which is defined as

$$\omega_{qp}(\vec{q})^2 = \vec{q}^2 + m^2 + \text{Re}\Pi(\omega_{qp}(\vec{q}), \vec{q}) , \quad (25)$$

moves to lower energies with respect to the free mass position for the D meson as density increases. As mentioned in Fig. 3, the presence of the $J = 1/2$ $\Sigma_c(2823)$ and $\Sigma_c(2868)$ resonances above threshold have an attractive effect at the DN threshold. In fact, those resonances can be clearly

TABLE II: DN and D^*N scattering lengths (fm)

	DN	D^*N
$J = 1/2 \ I = 0$	$0.001 + i \ 0.002$	$-0.44 + i \ 0.19$
(Born approx.)	$0.59 + i \ 0$	$1.82 + i \ 0$
$J = 1/2 \ I = 1$	$0.33 + i \ 0.05$	$-0.36 + i \ 0.18$
(Born approx.)	$0.20 + i \ 0$	$0.07 + i \ 0$
$J = 3/2 \ I = 0$		$-1.93 + i \ 0.19$
(Born approx.)		$0 + i \ 0$
$J = 3/2 \ I = 1$		$-0.57 + i \ 0.15$
(Born approx.)		$0.27 + i \ 0$

seen on the right-hand side of the quasiparticle peak. In the low-energy tail of the D spectral function, for energies around 1600 – 1650 MeV, we observe the $\Sigma_c(2556)N^{-1}$ and $\Lambda_c(2595)N^{-1}$ excitations. Moreover, other wider resonances are generated in the SU(8) model [57] and they combine to give the total D meson spectral function. In the SU(4) TVME models [38, 48, 49], the $J = 1/2 \ \Sigma_c(2800)N^{-1}$ fully mixes with the quasiparticle peak while the $\Lambda_c(2595)N^{-1}$ appears at the same energies as in our SU(8) model, as expected.

The quasiparticle peak of the D^* spectral function moves to higher energies with density and fully mixes with the sub-threshold $J = 3/2 \ \Lambda_c(2941)$ resonance. In the left-hand side of the peak we observe the mixing of $J = 1/2 \ \Sigma_c(2868)N^{-1}$ and $J = 3/2 \ \Sigma_c(2902)N^{-1}$ excitations. Other dynamically-generated particle-hole states appear for higher and lower energies, such as $J = 3/2 \ \Sigma_c(2554)N^{-1}$.

Density effects result in a broadening of the spectral functions as the collisional and absorption processes increase together with a dilution of the resonant-hole states. Finite momentum moves the quasiparticle peak to higher energies and softens the spectral function, according to the self-energy behavior of Fig. 3. This outcome is qualitatively similar to previous models for the D meson spectral function [35, 38, 47, 48, 49].

As already mentioned in one of the above references [49], the low-energy tail of the D meson spectral function due to resonant-hole states ($\tilde{Y}_c N^{-1}$) might help to understand the J/Ψ suppression in an hadronic scenario. However, it is unlikely that this lower tail extends with sufficient strength as far as the J/Ψ threshold to explain J/Ψ suppression only via the $D\bar{D}$ decay. A more plausible hadronic contribution for the J/Ψ suppression is the reduction of its supply from the excited charmonia, $\chi_{c\ell}(1P)$ or Ψ' , which may find in the medium other competitive decay channels [49]. Such a more broad scenario for the J/Ψ suppression has been pictured recently in thermal models [63]. On the other hand, the spectral function for the D and D^* mesons will influence the behavior of dynamically-generated hidden and open charm scalar resonances in nuclear matter, as already pointed out in Ref. [64].

Finally we study the properties of D and D^* mesons close to the DN and D^*N threshold. We first present in Table II results for the DN and D^*N effective interactions in free space. In particular, we give the $J = 1/2$ and $J = 3/2$ scattering lengths for $I = 0$ and $I = 1$,

$$a_{D(D^*)N}^{IJ} = -\frac{1}{4\pi} \frac{M_N}{\sqrt{s}} T_{D(D^*)N \rightarrow D(D^*)N}^{IJ} , \quad (26)$$

at $D(D^*)N$ threshold and with M_N the nucleon mass. For the DN effective interaction, we find that our $I = 0$ scattering length is negligible compared to the $I = 1$ one, in contrast to the SU(4) TVME model of Ref. [48] or the meson-exchange model of the Jülich group [40]. Moreover, our positive scattering lengths indicate the attractive behavior of the D meson self-energy close to

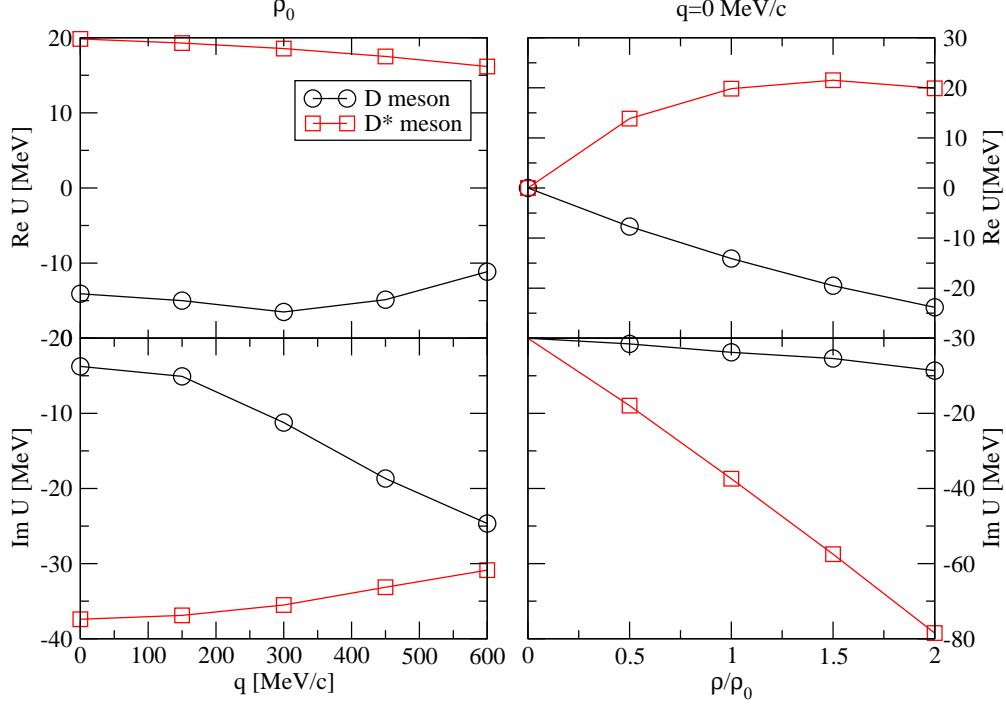


FIG. 5: D and D^* optical potentials as a function of the meson momentum $|\vec{q}|$ for $\rho = \rho_0$ (left panels) and as a function of ρ/ρ_0 for $|\vec{q}| = 0$ MeV/c (right panels).

threshold in contrast with the values of those previous references. The discrepancy with previous works has its origin in the different resonant-hole composition of the self-energy close to threshold. Moreover, as a new development, we also provide the D^*N scattering lengths. We note that the dominant repulsive contribution comes from the $J = 3/2$ partial wave.

Calculated scattering lengths come out radically different from those deduced within the Born approximation. This is not surprising because of the strong character of the meson-baryon interaction in the $C = 1$ sector, and the existence of resonances, which hint non-perturbative physics, close to the $D^{(*)}N$ threshold (in some cases they are placed even below it).

We can now define the D and D^* optical potentials in the nuclear medium as

$$U(\vec{q}) = \frac{\Pi(\omega_{qp}(\vec{q}), \vec{q})}{2\sqrt{m^2 + \vec{q}^2}}, \quad (27)$$

which, at zero momentum, can be identified as the in-medium shift of the D and D^* meson mass. The optical potential is shown in Fig. 5 for two cases: (i) real and imaginary parts as a function of the meson momentum $|\vec{q}|$ at ρ_0 (left panels) and (ii) real and imaginary parts as function of the density for $\vec{q} = 0$ MeV/c (right panels). The symbols indicate the calculated values for the optical potentials.

The mass shift at $\rho = \rho_0$ stays attractive for the D meson while becomes repulsive for the D^* meson with increasing momentum, in correspondence with the behavior of the quasiparticle peaks in Fig. 4. Similar values for the D meson potential were obtained for in-medium models of Refs. [35, 38, 47, 48, 49]. However, as explained in Fig. 4, the origin of the attraction can be traced back to a different resonant-hole contribution in the SU(4) models compared to the SU(8) case.

The imaginary part of the optical potential, which corresponds in module to half of the width of the spectral function at the quasiparticle peak, is reduced with momenta for the D meson

while increases for the D^* meson case. This can be understood by looking again at the spectral functions in Fig. 4 and analyzing the evolution of the quasiparticle peak and the dynamically-generated resonances with momenta. With increasing momentum, the quasiparticle peak of the D meson spectral function mixes completely with $\Sigma_c(2823)N^{-1}$ and $\Sigma_c(2868)N^{-1}$ and, therefore, the spectral function shows a wider shape. The quasiparticle peak of the D^* spectral function, however, moves away from $\Sigma_c(2941)N^{-1}$ and becomes slightly narrower.

With regard to the dependence on the density of the optical potentials at $|\vec{q}| = 0$ MeV/c, the dilution with density of the spectral functions give rise to the increase of the imaginary part of the optical potential for both D and D^* mesons. The real part stays attractive for the D meson while is repulsive for D^* meson. Then, we expect to find bound states for the D^0 -nucleus system [41]. Looking at the strength of the optical potential for density ρ_0 , we expect those states to be bound at most by 15 MeV and have half-widths lower than 4 MeV. Hence, we expect various states to be observable in different nuclei. It can be of interest to study the D^0 -nucleus spectrum, binding energies and widths predicted by the optical potential obtained here and compare it with predictions of other models. It is not clear that the D^+ -nucleus hadronic attraction will be able to overcome the Coulomb repulsion to provide similar bound states, that will be a subject of future research. Experiments to determine such a D^0 -nucleus bound states will be welcome.

IV. CONCLUSIONS

We have studied the properties of D and D^* mesons in symmetric nuclear matter within a simultaneous self-consistent coupled-channel unitary approach that implements the features of heavy-quark symmetry. The corresponding in-medium solution incorporates Pauli blocking effects, and the D and D^* meson self-energies in a self-consistent manner. In particular, we have analyzed the behavior of dynamically-generated baryonic resonances in the nuclear medium in the $C = 1$ and $S = 0$ sector within this SU(8) spin-flavor symmetric model and their influence in the self-energy and, hence, the spectral function of the D and D^* mesons. We have also obtained the D and D^* scattering lengths, and computed optical potentials for different momentum and density regimes. We have finally compared our results with previous SU(4) models [38, 40, 48, 49], paying a special attention to the renormalization of the intermediate propagators in the medium beyond the usual cutoff scheme.

The SU(8) model generates a wider spectrum of resonances with $C = 1$ and $S = 0$ content compared to the previous SU(4) models. While the parameters of both SU(4) and SU(8) models are fixed by the $(I = 0, J = 1/2)$ $\Lambda_c(2595)$ resonance, the incorporation of vectors mesons in the SU(8) scheme generates naturally $J = 3/2$ resonances, such as $\Lambda_c(2660)$, $\Lambda_c(2941)$, $\Sigma_c(2554)$ and $\Sigma_c(2902)$, which might be identified experimentally [62]. New resonances are also produced for $J = 1/2$, as $\Sigma_c(2823)$ and $\Sigma_c(2868)$, while others are not observed due to the different symmetry breaking pattern used in both models. The modifications of the mass and width of these resonances in the nuclear medium will strongly depend on the coupling to channels with D , D^* and nucleon content. Moreover, the resonances close to the DN or D^*N thresholds change their properties more evidently as compared to those far offshell. The improvement in the regularization/renormalization procedure of the intermediate propagators in the nuclear medium beyond the usual cutoff method has also an important effect on the in-medium changes of the dynamically-generated resonances, in particular, for those lying far offshell from their dominant channel, as the case of the $\Lambda_c(2595)$.

The self-energy and, hence, the spectral function of the D and D^* mesons show then a rich spectrum of resonant-hole states. The D meson quasiparticle peak mixes strongly with $\Sigma_c(2823)N^{-1}$ and $\Sigma_c(2868)N^{-1}$ states while the $\Lambda_c(2595)N^{-1}$ is clearly visible in the low-energy tail. The D^* spectral function incorporates the $J = 3/2$ resonances, and the $\Sigma_c(2902)N^{-1}$ and $\Lambda_c(2941)N^{-1}$

fully mix with the quasiparticle peak. As density increases, these $\tilde{Y}_c N^{-1}$ modes tend to smear out and the spectral functions broaden as the collisional and absorption processes increase. This broadening in dense matter might have important consequences for the dynamical generation of scalar resonances with hidden and open charm content [64] as well as for excited charmonium states for the experimental conditions expected in the PANDA and CBM experiments at FAIR [2]. This latter experimental scenario, however, requires the incorporation of finite temperature effects.

The behavior with density and momentum of the quasiparticle peaks is better visualized with the optical potentials. The D meson potential stays attractive while the D^* meson one is repulsive with increasing momentum and densities up to twice the normal nuclear matter one. The attractive and repulsive character of the DN and D^*N interactions close to threshold, respectively, was already observed in free space via the scattering lengths. In particular, the optical potentials with density do not follow the low-density approximation, as expected from the complicated resonant-hole structure of the self-energy. The imaginary part in both cases increases with density. However, the momentum dependence of the D and D^* meson potentials is distinct according to the position and behavior of the resonances close to threshold. Compared to in-medium SU(4) TVME models, we obtain similar values for the D meson real part of the potential but much smaller imaginary parts. This result can have important implications for the observation of D^0 -nucleus bound states. Work along this line is in progress.

Future work also includes the study of the influence of the Δ self-energy in the in-medium D and D^* self-energies as well as the inclusion of the width of the vector mesons in the meson-baryon channels. Moreover, finite temperature effects are mandatory for the analysis and interpretation of the data in the future CBM heavy-ion experiment at FAIR.

V. ACKNOWLEDGMENTS

C.G.R thanks L.L. Salcedo for useful discussions. L.T. wishes to acknowledge support from the “RFF-Open and hidden charm at PANDA” project from the Rosalind Franklin Programme of the University of Groningen (The Netherlands) and the Helmholtz International Center for FAIR within the framework of the LOEWE program by the State of Hesse (Germany). This research is supported by DGI and FEDER funds, under contracts FIS2008-01143/FIS and the Spanish Consolider-Ingenio 2010 Programme CPAN (CSD2007-00042), by Junta de Andalucía under contract FQM225. It is part of the European Community-Research Infrastructure Integrating Activity “Study of Strongly Interacting Matter” (acronym HadronPhysics2, Grant Agreement n. 227431) and of the EU Human Resources and Mobility Activity “FLAVIANet” (contract number MRTN-CT-2006-035482), under the Seventh Framework Programme of EU.

-
- [1] T. Matsui and H. Satz, Phys. Lett. B **178**, 416 (1986).
 - [2] <http://www.gsi.de/~fair/>
 - [3] M. Artuso *et al.* [CLEO Collaboration], Phys. Rev. Lett. **86**, 4479 (2001).
 - [4] R. Mizuk *et al.* [Belle Collaboration], Phys. Rev. Lett. **94**, 122002 (2005).
 - [5] R. Chistov *et al.* [BELLE Collaboration], Phys. Rev. Lett. **97**, 162001 (2006).
 - [6] B. Aubert *et al.* [BABAR Collaboration], Phys. Rev. Lett. **97**, 232001 (2006).
 - [7] B. Aubert *et al.* [BABAR Collaboration], Phys. Rev. Lett. **98**, 012001 (2007).
 - [8] R. Mizuk *et al.* [Belle Collaboration], Phys. Rev. Lett. **98**, 262001 (2007).
 - [9] N. Kaiser, P. B. Siegel and W. Weise, Nucl. Phys. A **594** (1995) 325.
 - [10] N. Kaiser, P. B. Siegel and W. Weise, Phys. Lett. B **362**, 23 (1995).
 - [11] E. Oset and A. Ramos, Nucl. Phys. A **635**, 99 (1998).

- [12] B. Krippa, Phys. Rev. C **58**, 1333 (1998); B. Krippa and J. T. Londergan, Phys. Rev. C **58**, 1634 (1998).
- [13] J. C. Nacher, A. Parreno, E. Oset, A. Ramos, A. Hosaka and M. Oka, Nucl. Phys. A **678**, 187 (2000).
- [14] U. G. Meissner and J. A. Oller, Nucl. Phys. A **673**, 311 (2000).
- [15] J. A. Oller and U. G. Meissner, Phys. Lett. B **500**, 263 (2001).
- [16] J. Nieves and E. Ruiz Arriola, Phys. Rev. D **64**, 116008 (2001).
- [17] T. Inoue, E. Oset and M. J. Vicente Vacas, Phys. Rev. C **65**, 035204 (2002).
- [18] M. F. M. Lutz and E. E. Kolomeitsev, Nucl. Phys. A **700**, 193 (2002).
- [19] C. Garcia-Recio, J. Nieves, E. Ruiz Arriola and M. J. Vicente Vacas, Phys. Rev. D **67**, 076009 (2003).
- [20] E. Oset, A. Ramos and C. Bennhold, Phys. Lett. **B527** (2002) 99.
- [21] A. Ramos, E. Oset and C. Bennhold, Phys. Rev. Lett. **89**, 252001 (2002).
- [22] D. Jido, J. A. Oller, E. Oset, A. Ramos and U. G. Meissner, Nucl. Phys. A **725**, 181 (2003).
- [23] L. Tolos, A. Ramos, A. Polls and T. T. S. Kuo, Nucl. Phys. A **690**, 547 (2001).
- [24] C. Garcia-Recio, M. F. M. Lutz and J. Nieves, Phys. Lett. B **582** (2004) 49 [arXiv:nucl-th/0305100].
- [25] J. A. Oller, J. Prades and M. Verbeni, Phys. Rev. Lett. **95**, 172502 (2005).
- [26] B. Borasoy, R. Nissler and W. Weise, Eur. Phys. J. A **25**, 79 (2005).
- [27] B. Borasoy, U. G. Meissner and R. Nissler, Phys. Rev. C **74**, 055201 (2006).
- [28] T. Hyodo, D. Jido and A. Hosaka, Phys. Rev. C **78**, 025203 (2008).
- [29] A. Ramos and E. Oset, Nucl. Phys. A **671** (2000) 481 [arXiv:nucl-th/9906016].
- [30] L. Tolos, A. Ramos and A. Polls, Phys. Rev. C **65**, 054907 (2002).
- [31] L. Tolos, D. Cabrera, A. Ramos and A. Polls, Phys. Lett. B **632**, 219 (2006).
- [32] L. Tolos, A. Ramos and E. Oset, Phys. Rev. C **74**, 015203 (2006).
- [33] L. Tolos, D. Cabrera and A. Ramos, Phys. Rev. C **78**, 045205 (2008).
- [34] D. Cabrera, A. Polls, A. Ramos and L. Tolos, arXiv:0903.1171 [nucl-th].
- [35] L. Tolos, J. Schaffner-Bielich and A. Mishra, Phys. Rev. C **70**, 025203 (2004).
- [36] J. Hofmann and M. F. M. Lutz, Nucl. Phys. A **763**, 90 (2005).
- [37] J. Hofmann and M. F. M. Lutz, Nucl. Phys. A **776**, 17 (2006).
- [38] T. Mizutani and A. Ramos, Phys. Rev. C **74**, 065201 (2006).
- [39] J. Haidenbauer, G. Krein, U. G. Meissner and A. Sibirtsev, Eur. Phys. J. A **33**, 107 (2007).
- [40] J. Haidenbauer, G. Krein, U. G. Meissner and A. Sibirtsev, Eur. Phys. J. A **37**, 55 (2008).
- [41] K. Tsushima, D.H. Lu, A.W. Thomas, K. Saito and R.H. Landau, Phys. Rev. C **59**, 2824 (1999).
- [42] A. Sibirtsev, K. Tsushima and A.W. Thomas, Eur. Phys. J. A **6**, 351 (1999).
- [43] A. Hayashigaki, Phys. Lett. B **487**, 96 (2000).
- [44] A. Mishra, E.L. Bratkovskaya, J. Schaffner-Bielich, S. Schramm and H. Stöcker, Phys. Rev. C **70**, 044904 (2004).
- [45] T. Hilger, R. Thomas and B. Kampfer, Phys. Rev. C **79**, 025202 (2009).
- [46] A. Mishra and A. Mazumdar, Phys. Rev. C **79**, 024908 (2009).
- [47] L. Tolos, J. Schaffner-Bielich and H. Stoecker, Phys. Lett. B **635**, 85 (2006).
- [48] M. F. M. Lutz and C. L. Korpa, Phys. Lett. B **633**, 43 (2006).
- [49] L. Tolos, A. Ramos and T. Mizutani, Phys. Rev. C **77**, 015207 (2008).
- [50] S. Sarkar, B. X. Sun, E. Oset and M. J. V. Vacas, arXiv:0902.3150 [hep-ph].
- [51] E. Oset, P. Gonzalez, M. J. V. Vacas, A. Ramos, J. Vijande, S. Sarkar and B. X. Sun, arXiv:0904.4804 [nucl-th].
- [52] E. Oset and A. Ramos, arXiv:0905.0973 [hep-ph].
- [53] C. García-Recio, J. Nieves and L. L. Salcedo, Phys. Rev. D **74**, 034025 (2006).
- [54] C. Garcia-Recio, J. Nieves and L. L. Salcedo, Phys. Rev. D **74**, 036004 (2006).
- [55] C. García-Recio, J. Nieves and L.L. Salcedo, Eur. Phys. J. **A31**, 499 (2007); Eur. Phys. J. **A31**, 540 (2007).
- [56] H. Toki, C. Garcia-Recio and J. Nieves, Phys. Rev. D **77**, 034001 (2008).
- [57] C. Garcia-Recio, V. K. Magas, T. Mizutani, J. Nieves, A. Ramos, L. L. Salcedo and L. Tolos, Phys. Rev. D **79**, 054004 (2009).
- [58] J. Nieves and E. Ruiz Arriola, Phys. Lett. **B455**, 30 (1999).
- [59] J. Nieves and E. Ruiz Arriola, Nucl. Phys. **A679**, 57 (2000).
- [60] J. Nieves, E. Oset and C. Garcia-Recio, Nucl. Phys. A **554**, 509 (1993).
- [61] J. Nieves, E. Oset and C. Garcia-Recio, Nucl. Phys. A **554**, 554 (1993).

- [62] W.-M. Yao et al., J. Phys. **G33**, 1 (2006).
- [63] A. Andronic, P. Braun-Munzinger, K. Redlich and J. Stachel, Phys. Lett. B **659**, 149 (2008).
- [64] R. Molina, D. Gamermann, E. Oset and L. Tolos, arXiv:0806.3711 [nucl-th].